This is an Authors' Accepted Manuscript of an article published in Control Engineering Practice. 16(3):356-364, March 2008, available online at:
http://www.sciencedirect.com/science/article/pii/S0967066107001104

Crane Feedback Control in Offshore Moonpool Operations

Saverio Messineo [a,*], Fabio Celani [b], Olav Egeland [a]

[a] *Centre for Ships and Ocean Structures (CeSOS)*
Norwegian University of Science and Technology NTNU
NO-7491, Trondheim, Norway

[b] *Dipartimento di Informatica e Sistemistica "Antonio Ruberti"*
Sapienza Università di Roma
Via Eudossiana 18, 00184 Roma, Italy

Abstract

A novel feedback controller for cranes employed in heavy-lift offshore marine operations is proposed. The control objective is to reduce the hydrodynamic slamming load acting on a payload at water-entry of moonpool operations; at the same time the values of the wire tension must be kept within acceptable bounds. The effectiveness of the proposed controller is shown experimentally; the experiments are performed on a scale model and show improvements with respect to a previous feedforward controller.

Key words: Mechanical systems, Marine systems, Feedback control methods, Observers, Output regulation

1 Introduction

In offshore marine operations there is often the necessity to safely install a payload on the seabed. This is motivated by the increasing trend to develop offshore oil and gas fields with all the processing equipment on the seabed and on the production well itself, as opposed to the more expensive solution of using a floating or a fixed production platform. Such a choice imposes severe requirements in terms of the safety and efficiency of the subsea intervention involved. This is witnessed by the considerable attention the field of ocean robotics has been given recently, see e.g. Silvestre and Pascoal (2007) and Caccia (2007). In particular, high subsea operability becomes a major issue in harsh sea conditions, when the higher possibility of losing or damaging the payload may cause a costly stop of the production and, most importantly, when the safety of the operators on board may be impaired as a consequence of loss of control of the payload.

A typical solution adopted by the marine industries consists in making use of an actively controlled crane which is placed on an offshore vessel and whose task is to lower the payload through a well in the ship hull referred to as "moon-pool". One of the critical phases is at water entry; indeed, when the payload is hit by the waves, it is subject to an impulsive hydrodynamic slamming force

* Corresponding author. Address: CeSOS, NTNU, Otto Nielsens veg 10, NO-7491 Trondheim, Norway; tel. +47 73595173; fax +47 73595528; e-mail: saverio@ntnu.no

which, in harsh sea conditions, can damage the payload. An additional quantity to monitor during the launch of the payload through the moonpool is the tension of the wire the payload is attached to; in fact, its minimum value must never be less than zero to avoid snatch loads that may break the wire, and its peak value must not exceed a safety limit. In addition, it is desirable to reduce the variations of the wire tension in order to decrease the wire's wear and tear.

In order to reduce the forces acting on the payload during the water-entry phase, Sagatun (2002) proposed a control strategy for the crane which was based on augmented impedance control.

Johansen, Fossen, Sagatun, and Nielsen (2003) proposed an alternative control strategy that was structured in two phases. The first phase, called "heave compensation", occurs when the payload is in the air and far enough from the moonpool. The goal is to have the payload move at an assigned constant vertical velocity in an earth-fixed reference frame. Achieving such a goal is beneficial in order to reduce the variations of the wire tension since the latter would be controlled to a constant value equal to the weight of the load. The second phase, called "wave synchronization", starts when the payload reaches the moonpool. As shown in Faltinsen and Zhao (1997), the impulsive hydrodynamic slamming force that affects the payload at water-entry increases as the relative velocity between the waves and the payload increases; consequently, the control objective of this phase is to lower the payload through the water-entry zone keeping such relative velocity constant and equal to a prescribed value. In each of the two phases, Johansen et al. (2003) proposed a feedforward compensator to achieve the control objectives since the main disturbances could be estimated reliably from sensors' data. The compensator was designed not taking into account the dynamics of the controlled system.

Skaare (2004) proposed a compensator that directly controls the wire tension rather than the velocity of the payload with respect to the waves.

Inspired by the idea of Johansen et al. (2003), a two-phase control strategy (heave-compensation, wave-synchronization) is proposed in this paper; however, here, in each of the two phases, a model-based feedback compensator is employed instead of the feedforward compensator presented in Johansen et al. (2003). In addition, here the transition between the two phases ends earlier than in Johansen et al. (2003).

It will be shown that in each of the two phases, the control objective translates into having a certain output variable track a reference signal and reject certain disturbances. A peculiar aspect of the control problem under consideration is that, in both phases, the controlled output is not measurable; however, to overcome such limitation, it is possible to design an observer that estimates the latter. As a result, the design methodology adopted in each of the phases consists of two steps. In the first step, pretending that the controlled variable is measurable, a compensator is designed. In the second step, an observer that estimates the controlled output is designed; the actual controller is obtained using the compensator of the first step with the controlled output replaced by its estimate.

The effectiveness of the proposed design, based on the certainty equivalence principle, is shown experimentally. The experiments are performed on a scale-model of a crane vessel with a moonpool. The experimental results show that the proposed feedback controller leads to significant improvements of the performance indicators compared to using the feedforward compensator of Johansen et al. (2003).

The rest of the paper is organized as follows. Section 2 describes the scale-model and its mathematical model. The controller is described in Section 3. The experiments are discussed in Section 4. Brief concluding remarks end the paper.

2 Scale-model and mathematical modeling

In this section, first a brief description of the crane vessel scale-model is given; then, a mathematical model is derived. The mathematical model will be used for control design.

2.1 Experimental Setup

The scale-model (see Fig. 1) consists of the following components; a floating vessel of dimensions 1.1 m $\times$ 0.67 m $\times$ 0.69 m; a 2.2 kW brushless asynchronous servo motor, attached to the floating vessel, with an internal PID speed-control loop; a spherical payload connected to the motor by a wire that goes over a pulley suspended by a spring; the spring is inserted in order to simulate the wire elasticity in a real crane vessel. The scale model is equipped with vertical accelerometers, in both the payload and the vessel, and with a force ring measuring the wire tension. The motor position is measured by means of an encoder. In the moonpool there is a wave meter attached to the vessel; the measure of the the conductivity between two parallel electrodes partly immersed in the water is used by the wave meter in order to determine the water level. The total mass of the crane-vessel is 157 kg.

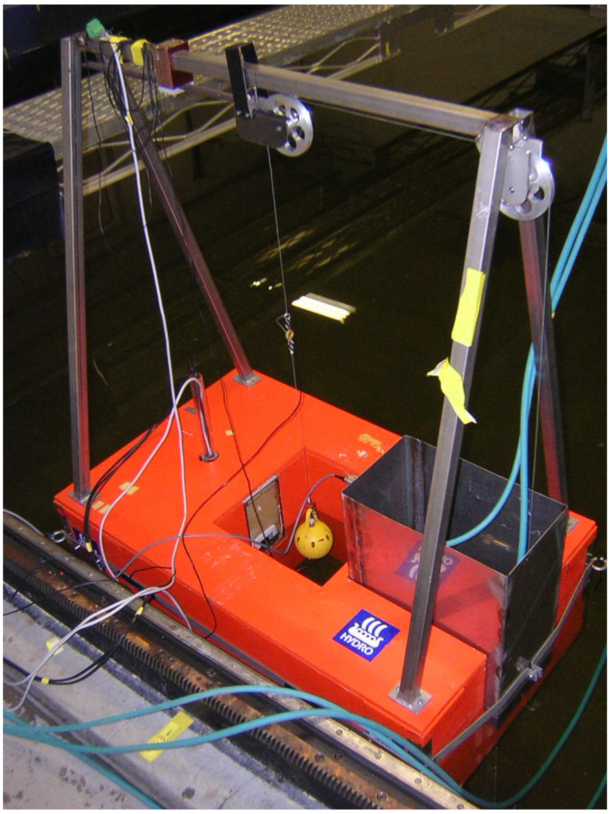

Fig. 1. Crane vessel scale model

A wave generator (a flap mounted at one end of the basin) is used to produce waves. The flap can move at different frequencies in order to produce different waves' spectra. The vessel is kept in a mean fixed position and heading with respect to the basin where it is placed.

The real-time control system is implemented on a target PC whose operating system is QNX 4.25. The target PC, equipped with an I/O card, communicates with an host PC via Ethernet. A Matlab / Simulink block diagram is developed on the host PC under Windows NT 4.0. By using Opal RT-lab 4.2 the block diagram is automatically converted into C-code and compiled on the target PC using the Watcom compiler. The results are presented online on the host PC using Labview 5.1. The sampling frequency is 20 Hz.

Further details on the experimental set-up can be found in Fossen and Sagatun

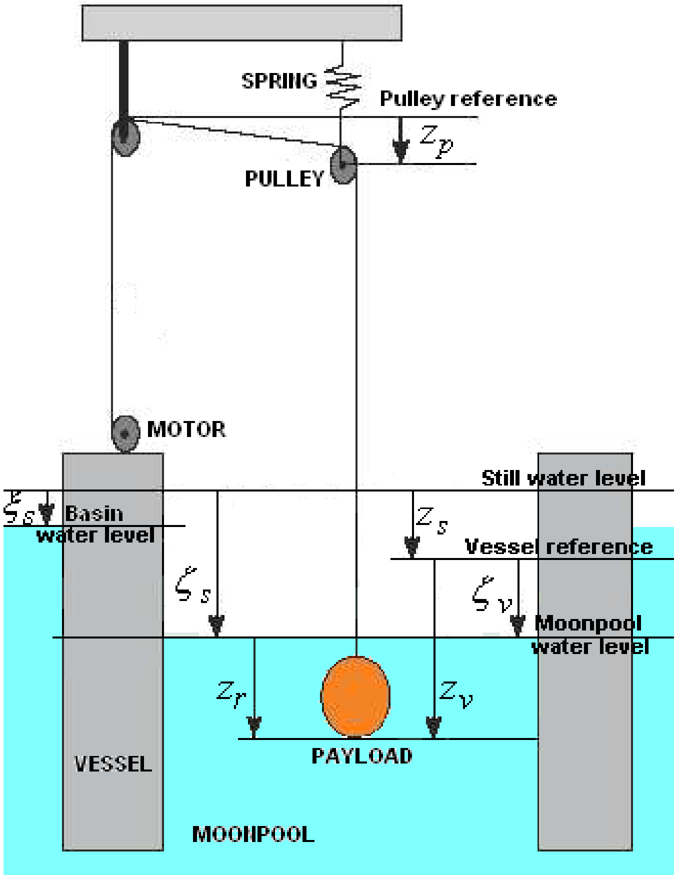

Fig. 2. Sketch of the scale-model

(2002).

2.2 Dynamics of the scale-model crane vessel

In deriving the mathematical model of the dynamics of the scale-model only the heave motion of the vessel and the vertical motion of the payload are considered. Consequently, effects from the vessel's roll and pitch motion are neglected. The wave profile is assumed to be uniform across the moonpool area.

In Fig. 2 a sketch of the experimental setup is shown along with a definition of references and coordinates. The still water level is, of course, fixed with respect to the earth. The vessel reference is attached to the vessel and is chosen so that when the vessel is still, it coincides with the still water level. The pulley reference is attached to the vessel and is chosen so that when the spring is at rest the center of the pulley lies on it.

The coordinates in Fig. 2 represent what follows

- z_v position of the load with respect to the vessel reference
- z_s position of the vessel reference with respect to the still water level
- ζ_s wave amplitude in the moonpool with respect to the still water level
- ζ_v wave amplitude in the moonpool with respect to the vessel reference
- z_p position of the pulley with respect to the pulley reference
- $z_r = z_v - \zeta_v$ position of the payload with respect to the moonpool water level
- ξ_s wave amplitude in the basin with respect to the still water level.

Let m be the payload mass, g the gravity acceleration, F_t the wire tension, and f_z the hydrodynamic force on the payload in the moonpool. Consider all coordinates and forces positive when they point downwards; then, the equation of motion of the payload is given by

$$m(\ddot{z}_v + \ddot{z}_s) = mg + f_z - F_t \ . \tag{1}$$

Let m_p be the mass of the pulley, d_p its damping coefficient, and k_p the spring stiffness; then, the equation of motion for the pulley is given by

$$m_p\ddot{z}_p + d_p\dot{z}_p + k_p z_p = F_t - m_p\ddot{z}_s \ . \tag{2}$$

Define

$$z_m \doteq z_v - z_p \ . \tag{3}$$

Note that z_m would be approximately equal to the position of the payload with respect to the vessel reference if the spring were at rest. As a result, if θ_m denotes the motor angular position, then the relation between z_m and θ_m can be modeled by $z_m = a_m\theta_m$ where a_m is a scalar that is determined by the geometric structure of the scale-model. Consequently, since the motor is equipped with an encoder that measures θ_m, z_m is indirectly measurable. Substituting (3) into (2) gives

$$m_p(\ddot{z}_v - \ddot{z}_m) + d_p(\dot{z}_v - \dot{z}_m) + k_p(z_v - z_m) = F_t - m_p\ddot{z}_s \, . \tag{4}$$

Denote with $\dot{z}_d$ the reference speed of the servo motor. A first-order model of the transfer function between $\dot{z}_m$ and $\dot{z}_d$ is adopted here and given by

$$\frac{\dot{z}_m}{\dot{z}_d} = \frac{\lambda}{s + \lambda} \tag{5}$$

with $\lambda = 33.33$ rad/s (see (Fossen and Johansen, 2001, p. 20)). The numerical values of the parameters in (1) and (4) have been determined in (Fossen and Johansen, 2001) through a system identification procedure; the obtained values are as follows; $m = 0.600$ kg, $m_p = 0.688$ kg, $d_p = 0.800$ kg s^{-1}, $k_p = 1046$ N m^{-1}.

The control input is given by $\dot{z}_d$; the measurable output is given by

$$y_m = (\ddot{z}_s \;\; \ddot{z}_s + \ddot{z}_v \;\; F_t \;\; \zeta_v \;\; z_m)^{\mathrm{T}} \, . \tag{6}$$

2.3 Hydrodynamic forces in the moonpool

Since the moonpool operates as a piston in a cylinder, the water vertical velocity can be assumed uniform from the water surface to the bottom of the moonpool. Consequently, when the payload is in the moonpool, f_z can be modelled by

$$f_z = -\rho g \nabla(z_r) - \rho \nabla(z_r)\ddot{z}_r - Z_{\ddot{z}_r}(z_r)\ddot{z}_r - \frac{\partial Z_{\ddot{z}_r}}{\partial z_r}(z_r)\dot{z}_r^2 - \frac{1}{2}\rho C_D A_{pz}\dot{z}_r\,|\dot{z}_r| - d_l \dot{z}_r \quad (7)$$

(see (Johansen et al., 2003, p. 721)). In (7), $\rho = 1000$ kg m^{-3} is the density of water; z_r is defined in Fig. 2 and represents the payload position with respect to the moonpool water level; $\nabla(z_r)$ is equal to the volume of the submerged part of the payload; $Z_{\ddot{z}_r}(z_r)$ is the position depended added mass of the payload; C_D is the drag coefficient; A_{pz} is the projected effective drag area of the payload in the vertical position; d_l represents the linear drag coefficient. Expressions and numerical values of the above quantities are reported in (Fossen and Johansen, 2001, pp. 7-8), and (Skaare, 2004, p. 104). The diameter of the payload is equal to $d = 0.09$ m.

In the experiments of Section 4 the desired value of $\dot{z}_r$ during the wave synchronization phase is $\dot{z}_r^* = 0.02$ m/s, and for control design purposes, it is useful to consider a linear approximation of (7) with respect to $z_r = d/2$, $\dot{z}_r = \dot{z}_r^*$, $\ddot{z}_r = 0$; such linear approximation is given by

$$f_z \cong k_1 - k_2 z_r - k_3 \dot{z}_r - k_4 \ddot{z}_r \quad (8)$$

where $k_1 = 1.28$ N, $k_2 = 77.04$ N/m, $k_3 = 1.48$ Ns/m, $k_4 = 2.86$ kg.

2.4 Dynamic model of crane vessel in heave

The heave motion of the crane vessel is represented by the following second order linear time-invariant differential equation

$$(m_v - Z_{\ddot{z}_s})\ddot{z}_s - Z_{\dot{z}_s}\dot{z}_s + \rho g A_{\dot{z}_s p} z_s = F_w\ . \quad (9)$$

Refer to (Fossen and Johansen, 2001, p. 3–5) for a description of the constant parameters m_v, $Z_{\ddot{z}_s}$, $Z_{\dot{z}_s}$, $A_{\dot{z}_s p}$. The natural frequency for z_s was determined experimentally as $\omega_h = 4.8$ rad/s (see (Johansen et al., 2003, p. 723)). The forcing term in (9) F_w represents the wave force in heave.

The wave amplitude in the basin ξ_s is modeled here as a stochastic process with power density spectrum equal to the so called JONSWAP spectrum (see (Fossen, 2002, p. 128)). This represents typical North Sea conditions that will be reproduced in the experiments described in Section 4. Furthermore, it is assumed that the transfer function $F_w(j\omega)/\xi_s(j\omega)$ is constant in the frequency range of interest; consequently, F_w is modeled as a stochastic process with the same JONSWAP power density spectrum of ξ_s up to a constant factor. The peak frequency of the JONSWAP spectrum is chosen equal to ω_h; such choice corresponds to the worst case scenario, i.e., the waves excite the resonance motion of the vessel; in such scenario, the power density spectrum of z_s in (9) possesses a peak at ω_h; for control design purposes, the latter power density spectrum is discretized to three harmonics so that

$$z_s = \sum_{i=1}^{3} A_i \sin(\omega_i t + \varphi_i) \tag{10}$$

where $\omega_1 = \omega_h$, $\omega_2 = 4.3$ rad/s (i.e. $\omega_2 = \omega_h - 0.5$ rad/s), $\omega_3 = 5.3$ rad/s (i.e. $\omega_3 = \omega_h + 0.5$ rad/s). In addition, it will be clear in Section 3 that the values of the amplitudes A_i's and of the phases φ_i's are irrelevant as far as the control design is concerned.

2.5 Moonpool Dynamics

The wave elevation inside the moonpool ζ_s can be represented by the following second-order differential equation

$$\ddot{\zeta}_s + d_m \dot{\zeta}_s + \frac{g}{h_m}\zeta_s = -\frac{1}{h_m}\frac{\partial \phi}{\partial t} \tag{11}$$

where d_m is the damping parameter, h_m is the still water depth of the moonpool, and ϕ is the wave velocity potential (see (Sagatun, 2002, p. 745)). The resonant frequency for ζ_s was determined experimentally as $\omega_m = 4.83$ rad/s (see (Johansen et al., 2003, p. 723)). Note that ω_m matches $\omega_h = 4.8$ rad/s almost exactly. Since ξ_s is modeled as a stochastic process that has a JONSWAP power density spectrum with peak at $\omega_h = 4.8$ rad/s, then it is reasonable to model the forcing term on the right hand side of (11) as a stochastic process with the same power density spectrum as ξ_s up to a constant factor. Then, considerations similar to those presented before for the heave motion of the vessel lead to the following model of the wave elevation inside the moonpool ζ_s

$$\zeta_s = \sum_{i=1}^{3} B_i \sin(\Omega_i t + \alpha_i). \tag{12}$$

Since $\omega_m \simeq \omega_h$, the Ω_i's are selected to be identical to the ω_i's of Section 2.4; it will become clear in Section 3 that such choice allows a reduction of the order of the compensator with respect to the situation where $\Omega_i \neq \omega_i \ \forall i$. It will also become clear that the values of the B_i's and α_i's are irrelevant for control design purposes.

3 Control design

As mentioned in the introduction, the control strategy adopted here consists of two phases. The first phase is called "heave compensation" and occurs when the payload is in the air and far enough from the moonpool. The second phase, called "wave synchronization", begins when the payload approaches the moonpool.

In this section the design of a compensator for each of the phases is presented. An important feature of each of the phases is that the controlled output is not measurable; however, it will be shown that it is possible to design an observer that estimates the latter. Then, the design of the compensator consists of two steps. In the first step, pretending that the controlled output is measurable, a synthesis based on the root-locus is performed in order to design a controller. In the second step, observers are designed in order to obtain an estimate of the controlled variable; the actual controller is then designed taking the compensator from the first step and replacing the controlled output with its estimate provided by the observer. The transition behaviour of the controller is discussed in section 3.4.

3.1 Heave Compensation

When the payload is in the air and far enough from the moonpool, the goal is to have the payload move at a constant prescribed velocity v_h^{ref} with respect to an inertial reference frame; in fact, if such goal is achieved, it is readily seen from (1) that, since $f_z = 0$, the wire tension F_t would be constant and equal to mg. Having constant F_t is beneficial to the wire because its wear and tear would be reduced. Thus, given such control objective, it is natural to set the velocity of the payload with respect to an inertial frame, i.e. $\dot{z}_v + \dot{z}_s$, as the controlled variable. However, this happens not to be feasible since it turns out that the system described by (1), (4), and (5) is not detectable from the output $\dot{z}_v + \dot{z}_s$. Then, a feasible way to proceed is as follows. Choose $z_v + z_s$ as the controlled variable and $v_h^{\mathrm{ref}} t + k_h$ as the reference trajectory where k_h is a constant. Then, let

$$\bar{g}(s) \doteq \frac{g}{s} \quad u_h \doteq \dot{z}_d \quad d_h(s) \doteq (m + m_p)s^2 + d_p s + k_p \; .$$

From (1), (4), and (5), it follows that

$$z_v(s) + z_s(s) = \frac{m_p s^2 + d_p s + k_p}{d_h(s)} \frac{\lambda}{s(s+\lambda)} u_h(s) + \frac{m}{d_h(s)} \bar{g}(s) + \frac{d_p s + k_p}{d_h(s)} z_s(s) \tag{13}$$

where $\bar{g}$ and z_s are regarded as disturbance inputs whereas u_h is the control input. Let $e_h = z_v + z_s - (v_h^{\mathrm{ref}} t + k_h)$ be the tracking error; then, pretending that $z_v + z_s$ is measurable, the control objective can be cast as follows; design a compensator $c_h(s) = u_h(s)/e_h(s)$ which stabilizes the closed-loop system and asymptotically steers to zero the error e_h in spite of the persistent disturbances g and z_s.

Recall that the model given by (10) is adopted for the disturbance z_s; then, using the internal model principle and the synthesis based on root-locus, the following compensator is derived

$$c_h(s) \doteq \frac{3000(s+3)^7}{s(s^2+\omega_1^2)(s^2+\omega_2^2)(s^2+\omega_3^2)} \; .$$

3.2 Wave synchronization

The wave synchronization phase starts when the payload is about to approach the moonpool. In this phase, the main objective is to reduce the impulsive hydrodynamic slamming force that affects the payload when the latter is hit by the waves. As shown in Faltinsen and Zhao (1997), the slamming force increases as the relative velocity between the waves and the payload $\dot{z}_v - \dot{\zeta}_v$ increases. Thus, the control objective is to lower the payload trough the water-entry zone keeping the quantity $\dot{z}_v - \dot{\zeta}_v$ constant and equal to a prescribed value v_w^{ref}. However, similarly to the previous phase, choosing $\dot{z}_v - \dot{\zeta}_v$ as the controlled variable would lead to a undetectable system; thus, in order to overcome such problem, the design proceeds choosing $z_v - \zeta_v$ as the controlled variable and $v_w^{\text{ref}} t + k_w$ as the reference trajectory where k_w is a constant. Then, let

$$\bar{g}_2(s) \doteq \frac{mg + k_1}{s} \quad u_w \doteq \dot{z}_d \quad d_w(s) \doteq (m + m_p + k_4)s^2 + (d_p + k_3)s + (k_p + k_2) \; .$$

From (1), (4), (5), and (8) it follows that

$$\begin{aligned} z_v(s) - \zeta_v(s) = {} & \frac{m_p s^2 + d_p s + k_p}{d_w(s)} \frac{\lambda}{s(s+\lambda)} u_w(s) + \frac{1}{d_w(s)} \bar{g}_2(s) \\ + & \frac{k_4 s^2 + k_3 s + k_2 - d_w(s)}{d_w(s)} \zeta_s(s) - \frac{(m + m_p + k_4)s^2 + k_3 s + k_2 - d_w(s)}{d_w(s)} z_s(s) \end{aligned} \tag{14}$$

where g, z_s and ζ_s are disturbance inputs, and u_w is the control input.

Consider the system described by (14), and suppose that the quantity $z_v - \zeta_v$ is measurable. Let $e_w = z_v - \zeta_v - (v_w^{\text{ref}} t + k_w)$ be the tracking error; then, the control objective is to find a controller $c_w(s) = u_w(s)/e_w(s)$ such that the closed-loop system is asymptotically stable and the error e_w decays asymptotically to zero in spite of the persistent disturbances g, z_s and ζ_s. Hence, recalling the models (10) and (12) for z_s and ζ_s respectively and using the same arguments as in section 2, it turns out that the compensator

$$c_w(s) \doteq c_h(s)$$

solves the problem under consideration.

3.3 Observers

As outlined before, estimates for the controlled outputs $z_v + z_s$ and $z_v - \zeta_v$ are required since the variables z_v and z_s are not measurable. In order to achieve this goal two observers are implemented; the first observer provides an estimate of z_v while the second observer provides an estimate of z_s.

The first observer is obtained as follows. Instead of considering all three equations (1) (4) (5) that describe the scale-model, it is enough to consider just equations (4) (5); in fact, for observer design purposes in such equations $\dot{z}_d$, F_t and $\ddot{z}_s$ can be regarded as inputs whereas $\ddot{z}_s + \ddot{z}_v$ and z_m can be regarded as outputs; this is feasible because on one hand $\dot{z}_d$ is the control input of the crane vessel, and on the other hand F_t, z_m and $\ddot{z}_s + \ddot{z}_v$ are measurable outputs.

Let $x_{p_1} = z_v$, $x_{p_2} = \dot{z}_v$, $x_{p_3} = \dot{z}_m$, $x_{p_4} = z_m$. Then, the resulting state-space representation of (4) and (5) is given by:

$$\begin{pmatrix} \dot{x}_{p_u} \\ \dot{x}_{p_d} \end{pmatrix} = \begin{pmatrix} A_{p_{11}} & A_{p_{12}} \\ A_{p_{21}} & A_{p_{22}} \end{pmatrix} \begin{pmatrix} x_{p_u} \\ x_{p_d} \end{pmatrix} + \begin{pmatrix} B_p \\ 0 \end{pmatrix} \begin{pmatrix} \dot{z}_d \\ F_t \\ \ddot{z}_s \end{pmatrix}$$

$$\begin{pmatrix} \ddot{z}_s + \ddot{z}_v \\ z_m \end{pmatrix} = \begin{pmatrix} C_p & \frac{k_p}{m_p} \\ 0 & 1 \end{pmatrix} \begin{pmatrix} x_{p_u} \\ x_{p_d} \end{pmatrix} + \begin{pmatrix} D_p \\ 0 \end{pmatrix} \begin{pmatrix} \dot{z}_d \\ F_t \\ \ddot{z}_s \end{pmatrix}$$

with

$$x_{p_u} = \begin{pmatrix} x_{p_1} & x_{p_2} & x_{p_3} \end{pmatrix}^T \quad x_{p_d} = \begin{pmatrix} x_{p_4} \end{pmatrix}$$

$$A_{p_{11}} = \begin{pmatrix} 0 & 1 & 0 \\ -\frac{k_p}{m_p} & -\frac{d_p}{m_p} & \frac{d_p}{m_p} - \lambda \\ 0 & 0 & -\lambda \end{pmatrix} \quad A_{p_{12}} = \begin{pmatrix} 0 \\ \frac{k_p}{m_p} \\ 0 \end{pmatrix} \quad B_p = \begin{pmatrix} 0 & 0 & 0 \\ \lambda & \frac{1}{m_p} & -1 \\ \lambda & 0 & 0 \end{pmatrix}$$

$$A_{p_{21}} = \begin{pmatrix} 0 & 0 & 1 \end{pmatrix} \quad A_{p_{22}} = \begin{pmatrix} 0 \end{pmatrix}$$

$$C_p = \begin{pmatrix} -\frac{k_p}{m_p} & -\frac{d_p}{m_p} & \frac{d_p}{m_p} - \lambda \end{pmatrix} \qquad D_p = \begin{pmatrix} \lambda & \frac{1}{m_p} & 0 \end{pmatrix} .$$

Note that the following pair is observable

$$\left(\begin{pmatrix} A_{p_{11}} & A_{p_{12}} \\ A_{p_{21}} & A_{p_{22}} \end{pmatrix} \begin{pmatrix} C_p & \frac{k_p}{m_p} \\ 0 & 1 \end{pmatrix}\right)$$

consequently, the following reduced-order Luenberger observer is designed

$$\dot{\hat{x}}_{p_u} = (A_{p_{11}} - KC_p)\hat{x}_{p_u} + \left((B_p - KD_p) \ \left(A_{p_{12}} - \frac{k_p}{m_p}K\right) \ K\right) \begin{pmatrix} \dot{z}_d \\ F_t \\ \ddot{z}_s \\ z_m \\ \ddot{z}_s + \ddot{z}_v \end{pmatrix}$$

$$\hat{z}_v = (1 \ 0 \ 0)\,\hat{x}_{p_u}$$

where

$$K = (0.00395 \ \ -0.00184 \ \ 0.57525)^{\mathrm{T}}$$

is such that $(A_{p_{11}} - KC_p)$ is Hurwitz. The sought estimate of z_v is then given by $\hat{z}_v$.

In order to compute an estimate of the controlled variable $z_v + z_s$, the problem of the estimation of z_s needs to be solved. To this end, notice from (10) that the variable z_s can be regarded as generated by the following unforced, linear, time-invariant system

$$\begin{aligned} \dot{w}_{z_0} &= S_{z_s} w_{z_s} \\ z_s &= C_0 w_{z_s} \end{aligned} \tag{15}$$

with

$$S_{z_s} = \mathrm{blkdiag}(S_1, S_2, S_3)$$

$$S_i = \begin{pmatrix} 0 & -\omega_i \\ \omega_i & 0 \end{pmatrix} \quad i = 1, 2, 3$$

$$C_0 = \begin{pmatrix} 1 & 0 & 1 & 0 & 1 & 0 \end{pmatrix}.$$

Note that the measurable variable $\ddot{z}_s$ can be expressed as follows

$$\ddot{z}_s = C_1 w_{z_s}$$

where

$$C_1 = \begin{pmatrix} -\omega_1^2 & 0 & -\omega_2^2 & 0 & -\omega_3^2 & 0 \end{pmatrix}.$$

Then, since the pair

$$\begin{pmatrix} S_{z_s} \\ C_1 \end{pmatrix}$$

is observable, the following Luenberger observer is designed

$$\dot{\hat{w}}_{z_s} = (S_{z_s} - K_{z_s} C_1)\hat{w}_{z_s} + K_{z_s} \ddot{z}_s$$

where

$$K_{z_s} = (-3.39 \;\; 2.24 \;\; 0.61 \;\; -2.10 \;\; 2.07 \;\; 0.87)^{\mathrm{T}}$$

is such that $(S_{z_s} - K_{z_s} C_1)$ is Hurwitz. Thus, the sought estimate $\hat{z}_s$ of z_s is given by

$$\hat{z}_s = C_0 \hat{w}_{z_s}\ .$$

3.4 Transition from Heave Compensation to Wave Synchronization

When the payload approaches the moonpool, the heave compensating feedback control u_h needs to turn into the wave synchronizing control u_w. The transition is here simply achieved through the blending factor α whose dependence on $\hat{z}_v$ is as follows

$$\alpha(\hat{z}_v) = \begin{cases} 0 & \text{if } \hat{z}_v < h_1 \\ \dfrac{1}{h_2 - h_1}(\hat{z}_v - h_1) & \text{if } h_1 \leq \hat{z}_v \leq h_2 \\ 1 & \text{if } \hat{z}_v > h_2 \end{cases} \tag{16}$$

where $h_1 = -0.20$ m and $h_2 = -0.15$ m are selected so that the transition ends before the payload hits the waves.

Blending u_h and u_w gives the following final control law

$$u = \alpha(\hat{z}_v)u_w + (1 - \alpha(\hat{z}_v))u_h$$

where $u \doteq \dot{z}_d$ and $\dot{z}_d$ denotes the speed commanded to the servo motor.

The transition proposed here ends earlier than the transition in (Johansen et al., 2003, p. 724); it is believed that this will help reducing the hydrodynamic slamming load acting on the payload at water entry.

4 Experiments

The controller proposed in this paper and the one in Johansen et al. (2003) were tested experimentally; in this section, the magnitudes of interests and the experimental conditions are described; then experimental results are presented and discussed.

4.1 Magnitudes of Interest and Experimental Conditions

The performance measures of interest are the following:

- **Hydrodynamic force.** As already mentioned, a critical phase of the underwater installation of a payload arises at water entry; the impulsive hydrodynamic slamming load that occurs when the payload hits the waves can seriously damage the latter when sea conditions are harsh; therefore, it is of interest to reduce such force; consequently, *the maximum of the absolute value of the hydrodynamic force affecting the payload* is reported. In addition, note that in (7) $Z_{\ddot{z}_r}(z_r)$ is constant when the payload is completely submerged; then, when the whole payload is submerged, if perfect wave synchronization were achieved, i.e. if $\dot{z}_r$ were constant, from (7) it follows that f_z would be constant; thus, in order to evaluate how effectively the wave synchronization control task is accomplished, *the standard deviation of the hydrodynamic force when the payload is completely submerged* is reported. In that regard note that from (1) it follows that $f_z = m(\ddot{z}_v + \ddot{z}_s) + F_t - mg$; then, the hydrodynamic force f_z is indirectly measurable since $(\ddot{z}_v + \ddot{z}_s)$ and F_t are measurable.
- **Wire tension.** The *minimum* value must never be negative in order to prevent high snatch loads that may break the wire; the *maximum* value must be within a safety bound; the standard deviation should be minimized in order to reduce the wear and tear of the wire. Furthermore, as already observed, if the heave compensation control goal was perfectly achieved,

then $\dot{z}_s + \dot{z}_v$ would be constant; as a consequence, from (1) it follows that F_t would be equal to the constant quantity mg. Thus, *the standard deviation of the tension for the sole heave compensation phase* is also reported.

The experiments were carried out generating waves in the basin; the waves are characterized by a JONSWAP spectrum (see (Fossen, 2002, p. 128)) with significant wave height $H_s = 0.02$ m and peak period $T_s = 1.3$ s; note that the corresponding peak frequency $\omega_s = 2\pi/T_s$ matches approximately the moonpool and vessel natural frequencies; consequently, a *resonant* behavior is induced in the motion of both the vessel and the water level in the moonpool; such experimental conditions represents the *worst case scenario* for the control problem under consideration.

The parameters of the reference signals in Subsections 3.1 and 3.2 were chosen as $v_h^{\mathrm{ref}} = v_w^{\mathrm{ref}} = 0.02$ m/s, $k_h = -v_h^{\mathrm{ref}} t_0 + z_m(t_0)$, and $k_w = -v_w^{\mathrm{ref}} t_0 + z_m(t_0)$ where t_0 is the start time of the control experiment.

4.2 Experimental results

For each of the two controllers, fifteen tests were carried out at the Marine Cybernetics Laboratory (MClab) of the Norwegian University of Science and Technology (NTNU) in Trondheim, Norway.

The data coming from the measures were filtered with a fourth order low-pass Butterworth filter with cutting frequency at 1.5 Hz. The filtering was performed in order to remove the high frequency components of the measurement noise. In the next subsection averaged results over the fifteen experimental runs are reported and discussed. The results are summarized in Table 1.

Magnitude	Fw	Fb	Imp
$\max(\lvert f_z \rvert)$	5.25 N	4.65 N	11.42 %
$\sigma(f_z)$	0.23 N	0.15 N	34.78 %
$\max(F_t)$	6.30 N	6.05 N	3.96 %
$\min(F_t)$	0.85 N	1.35 N	58.82 %
$\sigma_{HC}(F_t)$	0.22 N	0.14 N	36.36 %
$\sigma(F_t)$	2.06 N	1.70 N	17.47 %

Table 1

Performance comparison. Averaged results over fifteen experimental runs.

The symbols used in the table represent what follows

- Fw feedforward controller presented in Johansen et al. (2003)
- Fb feedback controller proposed in this paper
- Imp percentage improvement with the controller presented in this paper relative to the one presented in Johansen et al. (2003).
- $\max(|f_z|)$ maximum of the absolute value of the hydrodynamic force
- $\sigma(f_z)$ standard deviation of the hydrodynamic force when the payload is submerged
- $\max(F_t)$ maximum value of the wire tension
- $\min(F_t)$ minimum value of the wire tension
- $\sigma_{HC}(F_t)$ standard deviation of the wire tension during the heave compensation phase
- $\sigma(F_t)$ standard deviation of the wire tension calculated throughout the whole experiment.

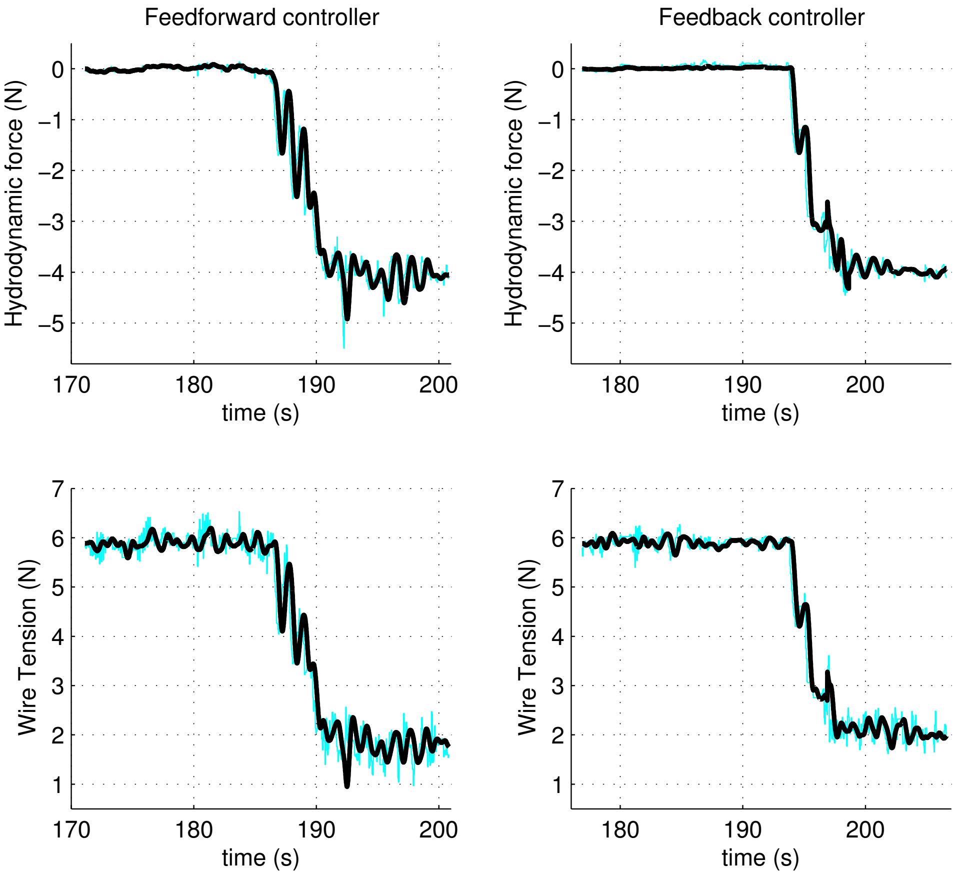

Fig. 3. Experimental results. Both raw data (thin lines) and filtered data (thick lines) are shown.

In Fig. 3 results from a single run out of the fifteen experimental runs are plotted for each compensator; the controller presented in Johansen et al. (2003) is labeled as "Feedforward controller", whereas the one proposed in this paper is labeled as "Feedback controller".

4.3 Discussion

The controller proposed here leads to a 11.25% reduction of the maximum of the absolute value of the hydrodynamic force; as a consequence, the probability that the payload could suffer damages is considerably reduced. Such an improvement is consistent with the value of the standard deviation of the hydrodynamic force affecting the completely submerged payload since such value is reduced from 0.23 N to 0.15 N; therefore, it can be stated that the proposed controller performs the wave synchronization task better than the one proposed in Johansen et al. (2003). Relevant improvements are registered with respect to the wire tension parameters. Specifically, the lower value reported for the standard deviation in the heave compensation phase, 0.14 N versus 0.22 N, highlights that the proposed controller attains the heave compensation objective better; this can also explain why the other values of interest regarding the wire tension are improved, too. Indeed, the wire-tension standard-deviation calculated throughout the whole experiment decreases from 2.06 N to 1.70 N; the maximum value decreases from 6.30 N to 6.05 N; the minimum value increases from 0.85 N to 1.35 N. This last performance is quite important, since avoiding negative values of wire tension is essential in order to prevent high snatch loads.

5 Conclusions

It is shown experimentally that the model-based feedback control proposed in this paper leads to better results than the feedforward control proposed in Johansen et al. (2003). Indeed, under the worst case scenario considered here, the controller presented in this paper achieves relevant improvements with respect to *all* the key values related to the hydrodynamic force and to the wire tension. The most important improvements are the ones achieved with respect to the values of both the slamming load and the minimum of the wire tension. In fact, by a practical point of view, this reduces the probability of a production stop due to the damage or loss of the payload.

Moreover, the decreased probability of a sudden wire break due to a high snatch load has the beneficial impact of increasing the safety of the operators on board.

A further improvement of the performances might be obtained by designing compensators that are robust with respect to parametric uncertainties. Such design for the problem under consideration will be the subject of future research.

6 Acknowledgements

This paper benefited from discussions with Prof. O. M. Faltinsen, Prof T. I. Fossen, Prof. A. Serrani, and Dr. B. Skaare. Moreover, the authors are grateful to Mr. S. Bertelli and Mr. T. Whal for their assistance during the experiments.

This work was funded by the Research Council of Norway under the Centre of Excellence scheme and by MUR under the program "Incentivazione alla mobilità di studiosi stranieri e italiani residenti all'estero".

References

Caccia, M., 2007. Vision-based rov horizontal motion control: Near-seafloor experimental results. Control Engineering Practice 15 (6), 703–714.

Faltinsen, O. M., Zhao, R., 1997. Water entry of ship sections and axisymmetric bodies. In: AGARD FDP and Ukraine Institute of Hydromechanics

Workshop on “High-Speed Body Motion in Water”, Report 827, Paper no. 24. Kiev, Ukraine, pp. 1–11.

Fossen, T. I., 2002. Marine control systems : guidance, navigation and control of ships, rigs and underwater vehicles. Marine Cybernetics, Trondheim.

Fossen, T. I., Johansen, T. A., 2001. Modelling and identification of offshore crane-rig system. Tech. Rep. 2001-12-T, Department of Engineering Cybernetics, NTNU, Trondheim, Norway.

Fossen, T. I., Sagatun, S. I., 2002. Vessel-crane moonpool specifications (hydrolab). Tech. rep., Department of Engineering Cybernetics, NTNU, Trondheim, Norway.

Johansen, T. A., Fossen, T. I., Sagatun, S. I., Nielsen, F. G., 2003. Wave synchronizing crane control during water entry in offshore moonpool operations - experimental results. IEEE Journal of Oceanic Engineering 28, 720–728.

Sagatun, S. I., 2002. Active control of underwater installation. IEEE Transactions on Control Systems Technology 10, 743–748.

Silvestre, C., Pascoal, A., 2007. Depth control of the infante auv using gain-scheduled reduced order output feedback. Control Engineering Practice 15 (7), 883–895.

Skaare, B., 2004. Control of loads through the wave zone in marine operations. Ph.D. thesis, NTNU, Trondheim, Norway.